Electrostatic model of atomic ordering in complex perovskite alloys

L. Bellaiche and David Vanderbilt
Department of Physics and Astronomy,
Rutgers University, Piscataway, New Jersey 08855-0849, USA
(June 23, 1998)

We present a simple ionic model which successfully reproduces the various types of compositional long-range order observed in a large class of complex insulating perovskite alloys. The model assumes that the driving mechanism responsible for the ordering is simply the electrostatic interaction between the different ionic species. A possible new explanation for the anomalous long-range order observed in some Pb relaxor alloys, involving the proposed existence of a small amount of Pb^{+4} on the B sublattice, is suggested by an analysis of the model.

PACS numbers: 64.60.Cn, 81.30.-t, 77.84.Dy, 77.84.-s

Complex insulating perovskite alloys are of great interest for their actual or potential uses mainly because of their exceptional dielectric and piezoelectric properties [1]. Examples are the so-called "super Q" mixed metal perovskites, such as $Ba(Zn_{1/3}Ta_{2/3})O_3$ (BZT) or $Ba(Mg_{1/3}Nb_{2/3})O_3$–$BaZrO_3$ (BMN–BZ), which can be used in high frequency applications because of their ultra-low losses at microwave frequencies [2,3]. Other examples are the "new" relaxor ferroelectric alloys, such as $Pb(Mg_{1/3}Nb_{2/3})O_3$–$PbTiO_3$ (PMN–PT) or $Pb(Zn_{1/3}Nb_{2/3})O_3$–$PbTiO_3$ (PZN–PT), which exhibit extraordinarily high values of the piezoelectric constants [4] and thus promise to improve the resolution and range of ultrasound and sonar listening devices [5].

An aspect that is not well understood about these complex materials is the compositional atomic ordering that occurs in some compounds and not in others, and the different kinds of long-range order (LRO) that can occur. For example, increasing progressively the bulk composition x in $(1-x)$ $Ba(Mg_{1/3}Nb_{2/3})O_3$ + x $BaZrO_3$ (BMN-BZ) leads to the following types of order for a final sintering temperature of 1640°C [2]: the so-called "1:2" ordering along the [111] direction for very small values of x (i.e., lower than 5%); then "1:1" ordering along [111] for compositions ranging from 5 to 25%; and finally, disordering for larger values of x.

The nature and strength of the compositional order may have crucial consequences for the desired properties of the material. For example, previous research has shown that the microwave loss properties of perovskite ceramics are very sensitive to the B-site cation order with the Q value improving with increasing degree of order [3,6]. Similarly, compositional fluctuations are believed to play a central role in the "relaxor" behavior in Pb-based perovskite alloys [7].

Previous pioneering theoretical work [8,9] has been partially successful in describing the ordering in some cases. In such models, the Coulomb interactions are included indirectly via a cluster expansion of finite range. While there is some justification for such an approach [10], the ordering sequences that occur in complex materials such as BMN-BZ did not emerge naturally, and thus the driving mechanism responsible for the ordering has remained somewhat obscure.

Motivated to resolve these problems, we decided to investigate a simple model that explicitly includes the long-range Coulomb interactions between ions. In this model, the energy is taken to be proportional to the electrostatic energy of an ideal system of ionic charges. We initially expected that this very simple model might need to be augmented with corrective covalent terms before it could provide a useful account of the different orderings seen in real materials. To our surprise, the minimal model by itself is remarkably successful. The purpose of this letter, then, is to show that this very simple model provides a systematic understanding of the complicated ordering behavior of complex perovskite alloys, thereby providing strong evidence that the Coulomb interaction between ions is the dominant factor in determining such ordering.

Our model assumes that the minimization of the electrostatic interactions between the different ions in the compounds leads to the LRO seen experimentally. The interaction energy in ABO_3 perovskite compounds is then expressed as

$$E = \frac{e^2}{2} \sum_{(l\tau)\neq(l'\tau')} \frac{Q_{l\tau} Q_{l'\tau'}}{\epsilon \, |\mathbf{R}_{l\tau} - \mathbf{R}_{l'\tau'}|} \,, \tag{1}$$

where $\mathbf{R}_{l\tau}$ is the position in the ideal cubic structure of the atom on site τ of cell l (τ=$\{$A,B,O_1,O_2,$O_3\}$), and ϵ is a dielectric constant providing some screening effects. While we find that this model can be successfully applied to other cases (see below), we first limit ourselves to divalent-A compounds having a common A atom on all A sites, and compositional freedom on the B site. In this case, we have $Q_{l,\mathrm{A}} = q_{\mathrm{A}} = +2$ and $Q_{l,\mathrm{O}} = q_{\mathrm{O}} = -2$ independent of l. Focusing on the B sites on which the alloying occurs, we can decompose $Q_{l,\mathrm{B}}$ as

$$Q_{l,\mathrm{B}} = q_{\mathrm{B}} + \Delta q_l \,, \tag{2}$$

where the *average* valence q_{B} is equal to +4 while Δq_l depends on l. In order to preserve overall charge neutrality,

the average $\overline{\Delta q}$ of Δq_l over all cells must vanish.

Substituting expression (2) for $Q_{l,\mathrm{B}}$ into Eq. (1), we can write $E = E_0 + E_1 + E_2$, where the subscript refers to the number of powers of Δq appearing in that term. Then E_0 is just a constant; it is the energy, within this model, of an ideal divalent-A and tetravalent-B perovskite compound. E_1 can be written as

$$E_1 = \frac{e^2}{2} \sum_l \Delta q_l \left[\sum_{l'\tau'} \frac{q_{\tau'}}{\epsilon \left| \mathbf{R}_{l\tau} - \mathbf{R}_{l'\tau'} \right|} \right] , \qquad (3)$$

but noting that the term in brackets does not actually depend on l and using $\overline{\Delta q} = 0$, it follows that E_1 vanishes. Thus the only term depending on the atomic order is

$$E_2 = \frac{e^2}{2} \sum_{l \neq l'} \frac{\Delta q_l \Delta q'_l}{\epsilon \left| \mathbf{R}_l - \mathbf{R}_{l'} \right|} . \qquad (4)$$

In fact, using $\mathbf{R}_l = \mathbf{l}a$ where a is the lattice constant,

$$E_2 = \frac{e^2}{2\epsilon a} \sum_{l \neq l'} \frac{\Delta q_l \Delta q'_l}{|\mathbf{l} - \mathbf{l}'|} . \qquad (5)$$

Eq. (5) demonstrates that our model can be reduced to focus only on the alloying sublattice (e.g., the B sublattice in the present case). Moreover, the model is parameter-free in the sense that $e^2/2\epsilon a$ defines a characteristic energy that will set the temperature scale on which ordering will occur.

In the following, we apply our model to various cases of divalent-A compounds with B-site alloying. We thus introduce a B-site-only notation. For example, $\mathrm{IV}_x\mathrm{IV}'_{1-x}$ will denote a homovalent binary alloy having tetravalent B atoms, e.g., $\mathrm{Pb}(\mathrm{Zr}_x\mathrm{Ti}_{1-x})\mathrm{O}_3$. In the same manner, $\mathrm{II}_{(1-x)/3}\mathrm{IV}_x\mathrm{V}_{2(1-x)/3}$ will indicate a heterovalent ternary, such as $(1-x)$ $\mathrm{Ba}(\mathrm{Mg}_{1/3}\mathrm{Nb}_{2/3})\mathrm{O}_3 + x$ BaZrO_3, which is the result of mixing a $\mathrm{II}_{1/3}\mathrm{V}_{2/3}$ heterovalent binary ($\mathrm{Ba}(\mathrm{Mg}_{1/3}\mathrm{Nb}_{2/3})\mathrm{O}_3$) with a tetravalent-B bulk (BaZrO_3).

In view of Eqs. (2) and (5), two points are immediately obvious. (i) The present model does not allow $\mathrm{IV}_x\mathrm{IV}'_{1-x}$ homovalent binary alloys to order, since Δq_l is identically zero in all cells l. This is in agreement with the experimental absence of LRO in homovalent alloys [11]. (ii) $\mathrm{II}_{1/2}\mathrm{VI}_{1/2}$ and $\mathrm{III}_{1/2}\mathrm{V}_{1/2}$ heterovalent binaries should behave much the same, since Δq_l consists in both cases of equal populations of charge $\pm n$, where $n = 2$ and 1 for $\mathrm{II}_{1/2}\mathrm{VI}_{1/2}$ and $\mathrm{III}_{1/2}\mathrm{V}_{1/2}$ alloys, respectively. Thus, these two cases really only differ in the magnitude of the effective energy scale factor $n^2e^2/2\epsilon a$. By computing the energy of a large variety of candidate structures and by performing Monte-Carlo simulations for small temperatures (see below), we determined that the ground-state (zero-temperature) structure predicted by the present model in these two cases is rocksalt, i.e., an alternation of $\pm n$ charged planes along the [111] direction. This is precisely the LRO observed experimentally in $\mathrm{Pb}(\mathrm{Sc}_{1/2}\mathrm{Ta}_{1/2})\mathrm{O}_3$ [7,12], $\mathrm{Pb}(\mathrm{In}_{1/2}\mathrm{Nb}_{1/2})\mathrm{O}_3$ [11], $\mathrm{Pb}(\mathrm{Yb}_{1/2}\mathrm{Ta}_{1/2})\mathrm{O}_3$ [13], $\mathrm{Pb}(\mathrm{Mg}_{1/2}\mathrm{W}_{1/2})\mathrm{O}_3$ [11], and $\mathrm{Pb}(\mathrm{Co}_{1/2}\mathrm{W}_{1/2})\mathrm{O}_3$ [11],

Similar calculations show that the present model also reproduces the ground-state 1:2 structure observed in many $\mathrm{II}_{1/3}\mathrm{V}_{2/3}$ heterovalent binaries, such as $\mathrm{Ba}(\mathrm{Mg}_{1/3}\mathrm{Nb}_{2/3})\mathrm{O}_3$ (BMN) [2], $\mathrm{Ba}(\mathrm{Zn}_{1/3}\mathrm{Ta}_{2/3})\mathrm{O}_3$ (BZT) [14,15], $\mathrm{Ba}(\mathrm{Mg}_{1/3}\mathrm{Ta}_{2/3})\mathrm{O}_3$ (BMT) [16], $\mathrm{Ba}(\mathrm{Sr}_{1/3}\mathrm{Ta}_{2/3})\mathrm{O}_3$ (BST) [16], $\mathrm{Ba}(\mathrm{Zn}_{1/3}\mathrm{Nb}_{2/3})\mathrm{O}_3$ (BZN) [17], $\mathrm{Ba}(\mathrm{Ni}_{1/3}\mathrm{Nb}_{2/3})\mathrm{O}_3$ (BNN) [18], and $\mathrm{Ca}(\mathrm{Ca}_{1/3}\mathrm{Ta}_{2/3})\mathrm{O}_3$ (CCT) [19]. That is, we do indeed find that the structure minimizing the electrostatic energy consists of one (111) layer of -2 relative charges (e.g., Zn-derived in BZN) alternating with two (111) layers of $+1$ relative charges (e.g., Nb-derived in BZN) along the [111] axis.

To extract further consequences from the model, it is necessary to solve for its thermodynamic behavior as a function of temperature. This is done using Metropolis Monte Carlo simulations [20] in which the (electrostatic) energy E_2 is given by Eq. (5). To be definite, we assign a=7.7 a.u. and ϵ=10. We normally limit ourselves to $6\times6\times6$ supercells since we checked that increasing the size of the calculations up to $12\times12\times12$ supercells does not change the results appreciably. We typically use a very large number of trial moves (up to $\sim 3\times10^7$ in transition regions) in order to obtain good statistics for each temperature. Since this corresponds to a large number ($\sim$35,000) of sweeps, the initial configuration is unimportant; it can either be chosen at random, or set to a given atomic order such as 1:2 or 1:1. To find the ground state, we first perform calculations at high temperature (e.g., 4,000K), and then very slowly decrease the temperature until reaching a structure for which no moves are accepted by the Monte-Carlo program.

Once the thermodynamic state corresponding to a given temperature has been reached, the search for LRO is done by calculating, from the Monte-Carlo outputs, the Fourier transform of the charge-charge correlation function,

$$\eta(\mathbf{k}) = \alpha \sum_{ll'} \Delta q_l \, \Delta q_{l+l'} \, \exp(-i\mathbf{k} \cdot \mathbf{l}') . \qquad (6)$$

Here α is a normalization factor, the sum runs over the charges in the B sublattice, and $\mathbf{k}$ is the wavevector in the Brillouin zone of the unit cubic cell. It can easily be demonstrated that $\eta(\mathbf{k})$ is directly proportional to the ensemble average of the square of the Fourier transform of the charge distribution. Thus, a large value of η at $\mathbf{k} = 2\pi(\frac{1}{2},\frac{1}{2},\frac{1}{2})$ corresponds to strong 1:1 LRO along the [111] direction, while a peak in η at $\mathbf{k} = 2\pi(\frac{1}{3},\frac{1}{3},\frac{1}{3})$ indicates 1:2 order along the [111] direction.

Figures 1(a-c) show the predicted behavior of $\eta(\mathbf{k})$ vs. tetravalent composition x at T=1000K for $\mathrm{III}_{(1-x)/2}\mathrm{IV}_x\mathrm{V}_{(1-x)/2}$, $\mathrm{II}_{(1-x)/2}\mathrm{IV}_x\mathrm{VI}_{(1-x)/2}$, and $\mathrm{II}_{(1-x)/3}\mathrm{IV}_x\mathrm{V}_{2(1-x)/3}$ heterovalent ternaries, respectively. We find that progressively increasing x in $\mathrm{III}_{(1-x)/2}\mathrm{IV}_x\mathrm{V}_{(1-x)/2}$ and $\mathrm{II}_{(1-x)/2}\mathrm{IV}_x\mathrm{VI}_{(1-x)/2}$ leads to

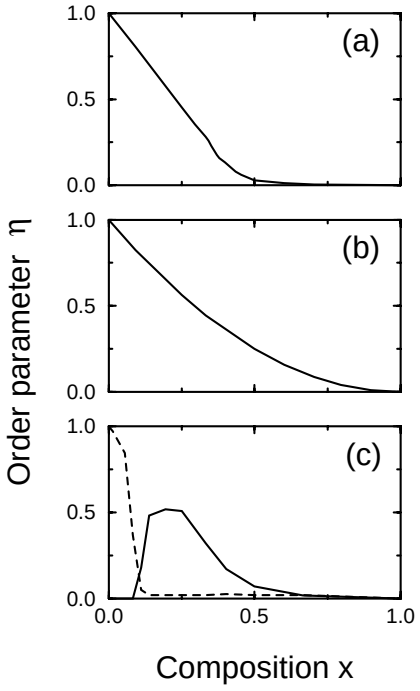

FIG. 1. Monte Carlo simulations of the long-range order parameter $\eta(\mathbf{k})$ *vs.* tetravalent atomic composition x for the model of Eq. (5), with $6\times6\times6$ supercells, a=7.7 a.u., ϵ=10, and T=1000K. Solid and dashed lines refer to 1:1 order $[\mathbf{k}=2\pi(\frac{1}{2},\frac{1}{2},\frac{1}{2})]$ and 1:2 order $[\mathbf{k}=2\pi(\frac{1}{3},\frac{1}{3},\frac{1}{3})]$, respectively. (a) $\mathrm{III}_{(1-x)/2}\mathrm{IV}_x\mathrm{V}_{(1-x)/2}$ ternaries. (b) $\mathrm{II}_{(1-x)/2}\mathrm{IV}_x\mathrm{VI}_{(1-x)/2}$ ternaries. (c) $\mathrm{II}_{(1-x)/3}\mathrm{IV}_x\mathrm{V}_{2(1-x)/3}$ ternaries.

a continuous transition from rocksalt-type order to a disordered state. This is consistent with the experimental findings in $(1-x)$ $Pb(Sc_{1/2}Ta_{1/2})O_3 + x$ $PbTiO_3$ [19,21]. We also predict that the 1:1 rocksalt order can survive in $\mathrm{II}_{(1-x)/2}\mathrm{IV}_x\mathrm{VI}_{(1-x)/2}$ alloys up to rather large x. This compositional difference between $\mathrm{III}_{(1-x)/2}\mathrm{IV}_x\mathrm{V}_{(1-x)/2}$ and $\mathrm{II}_{(1-x)/2}\mathrm{IV}_x\mathrm{VI}_{(1-x)/2}$ ternaries is due to the fact that the ground state energy of the latter is four times deeper than that of the former (for a given ϵ). Thus, quite a large number of tetravalent atoms is required to induce a disordered state in the $\mathrm{II}_{(1-x)/2}\mathrm{IV}_x\mathrm{VI}_{(1-x)/2}$ ternaries. We varied the temperature for the $\mathrm{III}_{(1-x)/2}\mathrm{IV}_x\mathrm{V}_{(1-x)/2}$ and $\mathrm{II}_{(1-x)/2}\mathrm{IV}_x\mathrm{VI}_{(1-x)/2}$ ternaries but found no qualitative changes (e.g., new phases), although naturally the transition from the ordered to the disordered phase is shifted to lower x with increasing T [22].

Figure 1(c) demonstrates that the atomic ordering predicted in $\mathrm{II}_{(1-x)/3}\mathrm{IV}_x\mathrm{V}_{2(1-x)/3}$ ternaries is even richer than in the previous two cases. We find 1:2 order along [111] for small x, then 1:1 rocksalt order for intermediate x, and finally a disordered state for even larger x. These predictions are in remarkable agreement with recent experimental observations of precisely this ordering sequence as a function of x in the microwave ceramics $(1-x)$ $Ba(Mg_{1/3}Nb_{2/3})O_3 + x$ $BaZrO_3$ [2], $(1-x)$ $Ba(Mg_{1/3}Ta_{2/3})O_3 + x$ $BaZrO_3$ [23], and $(1-x)$ $Ba(Zn_{1/3}Ta_{2/3})O_3 + x$ $BaZrO_3$ [24]. We find numerically that the critical value of x at which the crossover occurs from 1:2 to 1:1 order depends on the temperature used in the Monte-Carlo simulation, as well as on the value of the dielectric constant in Eq. (5). Increasing the temperature or increasing the dielectric constant leads to a decrease of this crossing composition. For example, keeping the lattice constant equal to 7.7 a.u. and using a dielectric constant of 15 yields a critical composition $x_c \sim 5\%$ for T=1000K. (A further increase in temperature or dielectric constant leads to alloy disorder even at small x composition.) Moreover, our calculations also confirm a suggestion based on experimental observations [2,23] for the structure responsible for the 1:1 order. Specifically, when we observe 1:1 order for $x < 25\%$, we find a rocksalt structure in which one sublattice is almost entirely occupied by pentavalent atoms, while the second sublattice is basically composed of the divalent and tetravalent atoms plus the remaining pentavalent atoms. The figure also indicates that the strongest 1:1 order occurs for a bulk composition of 25%, which is consistent with the experimental findings that the 1:1-order X-ray reflections seems to reach a maximum for $x = 0.25$ in $(1-x)$ $Ba(Zn_{1/3}Ta_{2/3})O_3 + x$ $BaZrO_3$ (BZT-BZ) [23].

On the other hand, there is a noteworthy exception to the ordering sequence shown in Fig. 1(c). Namely, in $\mathrm{II}_{(1-x)/3}\mathrm{IV}_x\mathrm{V}_{2(1-x)/3}$ ternaries for which the divalent A atom is Pb, the 1:2 ordering is *not* observed as $x \to 0$. Instead, these compounds exhibit weak 1:1 X-ray reflections all the way down to $x = 0$, as observed in $Pb(Mg_{1/3}Nb_{2/3})O_3$ (PMN) [25–27] and $Pb(Mg_{1/3}Ta_{2/3})O_3$ (PMT) [28]. As this appears to be at variance with our model, some explanation is clearly required. First, we note that our model predicts that the 1:2 and 1:1 ordering types are very close in free energy in $\mathrm{II}_{(1-x)/3}\mathrm{IV}_x\mathrm{V}_{2(1-x)/3}$ ternaries at small x. It is thus possible that in $\mathrm{II}_{1/3}\mathrm{V}_{2/3}$ binaries for which the A sublattice is occupied by Pb, some physical mechanism may occur that is responsible for triggering the 1:1 order in place of the 1:2 type. For example, a possible mechanism might be the covalency induced by the existence of short Pb–O bonds in the lead compounds [29]. The difference in covalency between Pb compounds and Ba compounds has been previously proposed to explain the difference in the ferroelectric behavior of $PbTiO_3$ and $BaTiO_3$ [30].

However, we wish to propose another possible mechanism for the existence of weak 1:1 order in PMN and PMT, related to the multivalent nature of the Pb atom. As is well known, Pb can be either divalent *or tetravalent*, in view of its s^2p^2 valence electronic configuration. Indeed, as much as 5% of Pb^{+4} has been experimentally reported in PMN [31]. These tetravalent Pb ions were initially thought to be sitting on the A sublattice of the perovskite alloy [31]. However, very recent experiments on $Pb(Sc_{1/2}Ta_{1/2})O_3$ (PST) films indicate the presence of some Pb^{+4} *on the B sublattice* of the perovskite struc-

ture [32]. Thus, we would like to raise the possibility that the Pb^{+4} atoms in PMN sit on the B sublattice. In this way, the application of Eq. (2) to PMN must recognize the existence of three species on the B sublattice: Mg^{+2}, Nb^{+5}, and a small number of Pb^{+4} (with relative charges -2, $+1$, and 0, respectively). The prediction of the present model for this case is again just that indicated in Fig. 1(c): only a small amount of Pb^{+4} (i.e., a small value of x) is needed to give rise to the weak 1:1 order observed in PMN and PMT. Interestingly, the existence of Pb^{+4} on the B sublattice of $II_{1/2}VI_{1/2}$ and $III_{1/2}V_{1/2}$ heterovalent alloys, e.g. $Pb(Co_{1/2}W_{1/2})O_3$ (PCW) and PST, will not lead to a change of ordering type. This is clearly shown in Figs. 1(a-b): whether x is small or exactly equal to zero, the 1:1 order is the only ordering predicted by our model for $II_{(1-x)/2}IV_xVI_{(1-x)/2}$ and $III_{(1-x)/2}IV_xV_{(1-x)/2}$ ternaries. In other words, unlike in PMN, the inclusion of a small amount of Pb^{+4} ions in PST may change the strength of the ordering but will not change the nature of the order itself.

While we have chosen to focus above on non-magnetic perovskite insulators with B-site substitutional disorder, our model is by no means limited to this case. In fact, the substitutional "impurity" may even be a vacancy. Denoting the latter by [ ], our model predicts that the ground state of $(Ca_{1/2}[\,]_{1/2})TaO_3$ should adopt the 1:1 rocksalt order of the Ca atoms and vacancies on the A sites. This is exactly the type of LRO observed experimentally in this system [19]. The extensions to magnetic perovskite insulators or to simultaneous A-site and B-site disorder, with possible incorporation of spin contributions or covalent effects into the model, are promising avenues for future work.

In summary, we have demonstrated that a purely ionic model is able to reproduce the various types of B-site compositional LRO observed in a wide variety of binary and ternary perovskite alloys. The remarkable success of this approach strongly suggests that the main driving mechanism responsible for the LRO occurring in heterovalent perovskite alloys is simply the electrostatic interaction between the different species. We also raise the possibility of a new mechanism in which a small amount of Pb^{+4} on the B sublattice may be responsible for (or at least contribute to) the weak 1:1-order X-ray reflections observed in some Pb relaxor systems.

This work is supported by the Office of Naval Research grant N00014-97-1-0048. We would like to acknowledge B.P. Burton and T. Egami for many very useful discussions.

[1] M.E. Lines and A.M. Glass, *Principles and Applications of Ferroelectrics and Related Materials* (Clarendon Press, Oxford, 1977).

[2] M.A. Akbas and P.K. Davies, *Solid State Chemistry of Inorganic Materials*, ed. P.K. Davies, A.J. Jacobson, C.C. Torardi, T and Vanderah, Proceedings **453**, 483 (1997).

[3] K. Matsumoto, T. Hiuga, K. Tanada and H. Ichimura, *Proceedings of the 8th IEEE International symposium on application of ferroelectrics*, 118 (1986).

[4] S.-E. Park and T.E. Shrout, *Journal of Materials Research Innovations*, in press (1997).

[5] R.F. Service, *Science* **275**, 1878 (1997).

[6] S. Kawashima, M. Nishida, I. Ueda and H. Ouchi, *J. Am. Ceram. Soc.* **66**, 421 (1983).

[7] N. Setter and L.E. Cross, *J . Appl. Phys.* **51**, 4356 (1980).

[8] B.P. Burton and R.E. Cohen, *Phys. Rev. B* **52**, 792 (1995).

[9] B.P. Burton, R.P. McCormack, B.H. Toby, and E.K. Goo, *Ferroelectrics* **194**, 187 (1997).

[10] G. Ceder, G.D. Garbulsky and P.D. Tepesch, *Phys. Rev. B* **51**, 11257 (1995).

[11] L. Eric Cross, *Ferroelectrics* **151**, 305 (1994).

[12] L. Eric Cross, *Ferroelectrics* **76**, 241 (1987).

[13] N. Yasuda and J. Konda, *Appl. Phys. Lett.* **62**, 535 (1993).

[14] A.J. Jacobson, B.M. Collins, and B.E.F. Fender *Acta Cryst. B* **32**, 1083 (1976).

[15] S.M. Allen and J.W. Cahn, *Acta Metall.* **20**, 27 (1972).

[16] R. Guo, A.S. Bhalla, and L.E. Cross *J. Appl. Phys.* **75**, 4704 (1994);

[17] U. Treiber and S. Kemmler-Sack, *J. Sol. State Chem* **43**, 51 (1982).

[18] Kim, *Ferroelectrics* **173**, 125 (1995).

[19] B.P. Burton, private communication.

[20] N. Metropolis *et al*, *J. Chem. Phys.* **21**, 1087 (1953).

[21] J.R. Giniewicz, A.S. Bhalla, and L.E. Cross *Ferroelectrics Letters* **12**, 35 (1990).

[22] In fact, Figs. 1(a) and (b) can be regarded as giving the results for the $II_{(1-x)/2}IV_xVI_{(1-x)/2}$ and $III_{(1-x)/2}IV_xV_{(1-x)/2}$ ternaries at T=4000K and T=250K respectively.

[23] L. Chai, M.A. Akbas, P.K. Davies, and J.B. Parise, *Materials Research Bulletin* Pergamon **32** (1997).

[24] P.K. Davies, J. Tong and T. Negas, *Journal of American Society* **80**, 1727 (1997).

[25] E. Husson, *Mat. Res. Bull.* **25**, 539 (1990).

[26] E. Husson, *Mat. Res. Bull.* **23**, 357 (1988).

[27] J. Chen, *J. Am. Cer. Soc.* **72**, 593 (1989).

[28] M.A. Akbas and P.K. Davies, *Journal of Materials Research.* **12**, 2617 (1997).

[29] T. Egami, S. Teslic, W. Domowski, P.K. Davies and I.-W. Chen, *submitted* (1997).

[30] R.E. Cohen, *Nature* **358**, 136 (1992).

[31] H.D. Rosenfeld and T. Egami, *Ferroelectrics* **150**, 183 (1993).

[32] R.W. Whatmore, Z. Huang, M. Todd, *J. Appl. Phys.* **82**, 5686 (1997);